Lateral Control Design of an Autonomous Land Vehicle Using RTK-DGPS

Hyung Gyu Park, Jae Heon Ryu
and Seong Taek Hwang
Department of Mechanical and
Intelligent Systems Engineering
Pusan National University
Busan, 609-735, KOREA

Man Hyung Lee
School of Mechanical Engineering,
Pusan National University
Busan, 609-735, KOREA

Abstract

This paper describes the development of the H_∞ lateral control system for an autonomous ground vehicle in a limited area using the RTK-DGPS (Real Time Kinematic - Differential Global Positioning System). Before engaging in autonomous driving, map data are acquired by using the RTK-DGPS. The data are the reference trajectory for autonomous vehicles. The navigation system with the map data computes the reference yaw angle of the vehicle using its present position and next position. Also, the yaw angle of the vehicle is controlled by the H_∞ controller. A prototype of the autonomous vehicle by the navigation method is developed. In addition, the performance of the vehicle is evaluated by experiment. The experimental results show that the H_∞ controller and the RTK-DGPS based navigation system can sufficiently track the map at low speed. We expect that this navigation system can be made more accurate by augmenting other sensors.

1 Introduction

Research centered on ITS (Intelligent Transportation System) and PATH (Partners for Advanced Transit and Highways) has led to the development of the autonomous vehicle. Generally, it has been realized using MR sensors and vision sensors, among other technologies. Though the autonomous vehicle was created in part by using them, it is difficult to operate autonomous vehicles in all conditions [1]. For example, if we use MR sensors, we must mark magnet points on the road and stochastic error occur. With vision sensors, the problem is that they are sensitive to weather conditions or light [2]. Now, concerning about the navigation systems by using the absolute coordinate system has progressed [3]. So, we realized an autonomous vehicle using the absolute coordinate system with an RTK-DGPS (Real Time Kinematic-DGPS)

Generally, a differential GPS has been used for improving the accuracy of GPS. All the DGPS reference stations have transmitters to forward the error factors to DGPS receivers by radio or other methods, which gives the information to the GPS receiver so it can use the data to correct its own measurements and calculations. This differential correction technique applies to GPS receivers performing code-phase navigation.

When a receiver navigates in carrier-phase mode, it is measuring a different GPS observable, namely the GPS carrier wave. In order to obtain high accuracy with carrier-phase measurements, it is necessary to compute the number of GPS wavelengths between the roving GPS receiver's antenna and the satellites using the information (i.e., carrier-phase measurements) from a base receiver. This technique yields accuracy to the cm-level in dynamic environments called RTK-DGPS. So, the method is used to make a digital road map and computes vectors for navigation.

In this paper, the H_∞ control by the feedback of the yaw angle error was used to design a robust lateral control against modeling uncertainty [4]. Furthermore, its property is compared that of the PID controller.

2 Lateral Control

2.1 Lateral Vehicle Model

This section considers a classic linearized bicycle model with two degrees of freedom for the lateral and yaw dynamics of a vehicle. We used the PATH car model (Fig. 1) in order to design controller. Because our main interest is with steering control, we ignored the roll, pitch, and vertical movement of the vehicle. And if we suppose that the vehicle runs on a flat road, we can regard the lateral slip angle and the yaw angle as small [5]. Also, if the speed of the vehicle is constant, the complex car

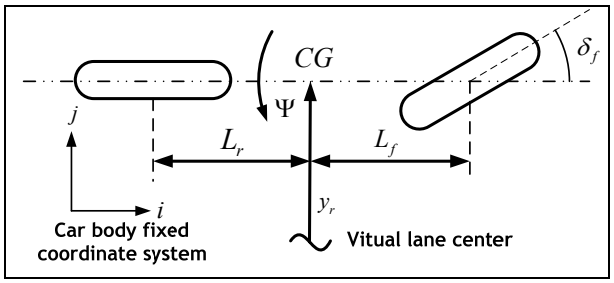

Fig. 1 Integration concept of operation

model equation can be simplified. The curvature of the road was not considered in this study for simplifying the model, since the effect of the curvature on vehicle control at the low speed and in the large curvature is less than that of other uncertainties and external disturbances.

The linearized dynamic equation can be simple, as follows:

$$\frac{\mathrm{d}}{\mathrm{dt}}\begin{bmatrix} y_r \\ \dot{y}_r \\ \Psi_r \\ \dot{\Psi}_r \end{bmatrix} = \begin{bmatrix} 0 & 1 & 0 & 0 \\ 0 & \frac{A_1}{V} & -A_1 & \frac{A_2}{V} \\ 0 & 0 & 0 & 1 \\ 0 & \frac{A_3}{V} & -A_3 & \frac{A_4}{V} \end{bmatrix} \begin{bmatrix} y_r \\ \dot{y}_r \\ \Psi_r \\ \dot{\Psi}_r \end{bmatrix} + \begin{bmatrix} 0 \\ B_1 \\ 0 \\ B_2 \end{bmatrix} \delta_f , \tag{1}$$

where A_1, A_2, A_3, A_4, B_1, and B_2 are defined as

$$A_1 = -\frac{C_f + C_r}{m}, \qquad A_2 = -\frac{(C_f L_f - C_r L_r)}{m},$$

$$A_3 = \frac{(-C_f L_f + C_r L_r)}{J}, \quad A_4 = -\frac{(C_f L_f^2 + C_r L_r^2)}{J},$$

$$B_1 = \frac{C_f}{m} \quad \text{and} \quad B_2 = \frac{C_f L_f}{J}.$$

The front wheel steering actuator is assumed to be dominated by the first order delay.

$$\theta_m = \frac{1}{T_m s + 1} u_f , \tag{2}$$

where, T_m is the time constant of the motor and u_f is the control input and θ_m is the motor (or steering wheel) angle.

The steering system from the motor (or steering wheel) angle θ_m to the wheel angle δ_f is modeled as a gear with the gear ratio of n. So, δ_f is given by

$$\delta_f = n\theta_m . \tag{3}$$

Combining the dynamics of the actuator and the vehicle dynamics, a 5th order state space model with states $X = \begin{bmatrix} y_r & \dot{y}_r & \Psi_r & \dot{\Psi}_r & \theta_m \end{bmatrix}^T$ is obtained as follows:

$$\dot{X} = \begin{bmatrix} 0 & 1 & 0 & 0 & 0 \\ 0 & \frac{A_1}{V} & -A_1 & \frac{A_2}{V} & B_1 \cdot n \\ 0 & 0 & 0 & 1 & 0 \\ 0 & \frac{A_3}{V} & -A_3 & \frac{A_4}{V} & B_2 \cdot n \\ 0 & 0 & 0 & 0 & -\frac{1}{T_m} \end{bmatrix} X + \begin{bmatrix} 0 \\ 0 \\ 0 \\ 0 \\ \frac{1}{T_m} \end{bmatrix} u_f . \tag{4}$$

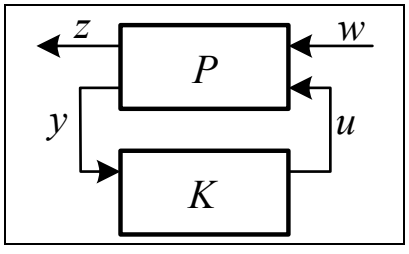

Fig. 2 The basic block diagram of H_∞ controller

2.2 Lateral Control of an Autonomous Vehicle

Fig. 2 is general a block diagram of H_∞ control. The components of w are all the exogenous inputs to the system [6]. Typically, these consist of disturbances, sensor noise reference commands and fictitious signals that drive frequency weights and models of the uncertainty in the dynamics of the system. The components of z are all the variables we wish to control like the tracking errors and the actuator signals. The inputs generated by the controller are denoted u. The sensor measurements that are used by the feedback controller are denoted y.

The generalized plant P, which is assumed to be linear and time-invariant, contains all the information a designer would like to incorporate into the synthesis of the controller, K. System dynamics, models of the uncertainty in the system's dynamics, frequency weights to influence the controller synthesis, actuator dynamics, sensor dynamics, and implementation hardware dynamics are all included in P.

The relation of the variable z and the exogenous input is $z = T_{zw} w$. So, the H_∞ control is represented as

$$\left\| T_{zw} \right\|_\infty \le \gamma . \tag{5}$$

The H_∞ control is represented as (6) with the method of Glever and Doyle [7].

$$\left\| \begin{matrix} W_1 S \\ W_3 T \end{matrix} \right\|_\infty \le \gamma . \tag{6}$$

Regarding the mixed-sensitivity problem, W_1 and W_3 are weighting functions for improving performance of the system. In addition, S and T are the sensitivity function and the loop transfer function of the system, respectively. Based on the time domain performance specifications, the corresponding requirements in a frequency domain in terms of the bandwidth ω_b and the peak sensitivity M_s can be determined. This assumes that the steady state error of the step response ε has to

satisfy $|W_1(0)| \geq 1/\varepsilon$. A possible choice of W_1 can be obtained by modifying the weighting function as follows:

$$W_1 = \frac{s/M_S + \omega_b}{s + \omega_b \varepsilon}. \quad (7)$$

Additionally, the magnitude of $|KS|$ in the low-frequency range is essentially limited by the allowable cost of control effort and saturation limit of the actuators; hence, in general, the maximum gain M_T of KS can be fairly large, while the high-frequency gain is essentially limited by the controller bandwidth (ω_{bc}) and the sensor noise frequencies. A candidate weight W_3 would be

$$W_3 = \frac{s + \omega_{bc}/M_T}{\varepsilon_1 s + \omega_{bc}} \quad (8)$$

for a small $\varepsilon_1 > 0$.

Fig. 3 is the bode plot of each weighting function.

3 Navigation Algorithm

Fig. 4 shows the target points are determined using map data. When the unmanned vehicle navigates the road, it compares current position with map data. However, the navigation system cannot compare all data for searching target points. So, it calculates maximum moving distance r of the vehicle by using velocity of the vehicle until acquiring the next set of RTK-DGPS data. It compares the current position with maximum distance position M_{n+2} within the circle that has a radius r. It calculates the yaw reference $|\psi_{ref}|$ by the dot product of vectors. It uses the prior position P_{t-1}, the current position P_t and the target position M_{n+2}, which is shown in equation (9) as follows:

$$|\psi_{ref}| = \cos^{-1} \frac{\overrightarrow{P_{t-1}P_t} \cdot \overrightarrow{P_tM_{t+2}}}{|\overrightarrow{P_{t-1}P_t}| \cdot |\overrightarrow{P_tM_{t+2}}|}. \quad (9)$$

Also, the sign of direction is solved by using the sign of the cross product of vectors. So, we can acquire ψ_{ref} as follows:

$$\psi_{ref} = sign(\vec{k}(P_{t-1}P_{t_x} \times P_tM_{t+2_y} - P_{t-1}P_{t_y} \times P_tM_{t+2_x})) \times |\psi_{ref}|. \quad (10)$$

For determining the target point, r is calculated by using velocity V of the vehicle, sampling time (t) of the RTK-DGPS and α, the coefficient considered curvature of the road. α is used for determining the proper target point. If target points are calculated at 1 second intervals, the variation of yaw severely increases. So, angle data λ of the vectors are added to the path data by post-processing. The data are calculated using $n-1$ th, n th and $n+1$ th data in the path data. The coefficient α is acquired by using equation (11). It is optimized by simulation and experiments as follows:

$$\begin{cases} \lambda > 0.1\ radian, & \alpha = 1 \\ \lambda < 0.1\ radian, & \alpha = 180\lambda^2 - 37\lambda + 3. \end{cases} \quad (11)$$

4 Experiment

4.1 Experimental System

The experiment vehicle is SPORTAGE of KIA motors. The RTK-DGPS system is from the Z-family of Ashtech. The accuracy of the synchronized RTK mode is 0.5cm+1ppm. In addition, the maximum position output rate at the remote receiver is 1Hz. The communication between the base station and the remote station in the vehicle was accomplished by using a PDL (Positioning Data Link) system that uses an RF connection. Also, we used the digital compass of Robot electronics. Its absolute error is 3˚, with a resolution of 0.1˚. The navigation computer was PXI-1002 from National Instrument. Finally, the navigation software was coded

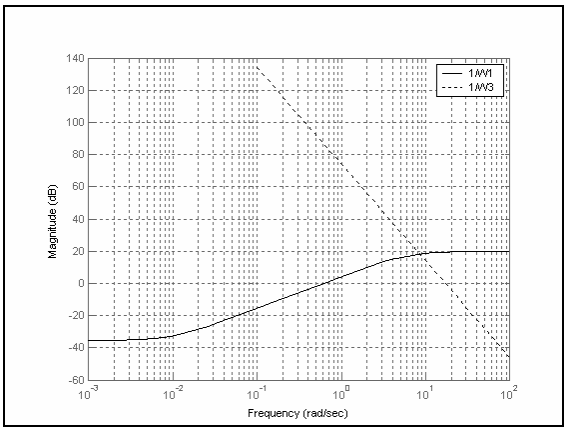

Fig. 3 Selected weighting functions

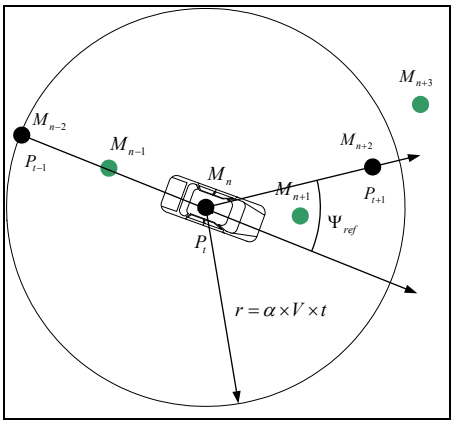

Fig. 4 Navigation concept

by using LabVIEW 6.1.

4.2 Experiment Results

The width of the test road was a minimum 3.6 m and the vehicle width was 1.735 m. Before the test, the path data were acquired by using the RTK-DGPS. Fig. 8 is the path data. The full lap of it was 160 m.

The velocity of the vehicle is about 2.778 m/s (about 10 km/h). Fig. 6 shows the test results when the parameter is similar to that used in designing the controller. In Fig. 7, the velocity and mass of the vehicle are changed in the test driving condition. This was done in order to compare performance of each controller considering modeling uncertainty. The performance of the H_∞ controller is more robust than a PID controller for a change of system parameters. Table 1 presents the maximum and mean of the errors of each experiment.

5 Conclusion

In this paper, the real vehicle was implemented to verify the performance of a proposed lateral control and a simple navigation algorithm. To control the yaw of the vehicle, an H_∞ control algorithm was introduced. To cope with the sensor noise and the modeling uncertainty, a robust lateral controller was designed by the feedback of the yaw angle error of the vehicle.

The position and attitude of the vehicle was calculated by using the RTK-DGPS and a digital compass. The vehicle was steered by DC motors which were controlled by a real time module. The experimentation for the real scale vehicle showed that the proposed lateral controller improved the tracking performance.

We also considered current related work concerned with improving the precision of dead reckoning by correction of the diameters of tires. In such cases, the vehicle navigates for a longer time by dead reckoning in an urban canyon environment. We expect such applications will be useful in the future to create a wheel chair system for blind.

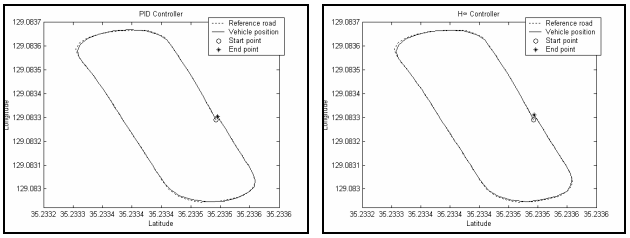

(a) PID Controller (b) H_∞ Controller

Fig. 5 Trajectories for each controller

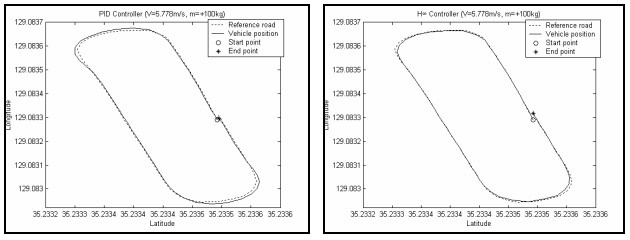

(a) PID Controller (b) H_∞ Controller

Fig. 6 Trajectories for each controller(+2m/s,+100kg)

Table 1. Results of driving test

Test result	Maximum error[m]	Mean error[m]
PID	0.447	0.276
H_∞	0.521	0.220
PID(+2m/s,+100kg)	0.914	0.483
H_∞ (+2m/s,+100kg)	0.732	0.310

Acknowledgment

This work was supported by the Brain Korea 21 Project.

Reference

[1] Huei, P., Wei-Bin, Z., Alan, A., Ye, L., Thomas, H., Peter, D., Masayoshi, T., and Steven, S, Experimental Automatic Lateral Control System for an Automobile, PATH Research Report, 1992.

[2] Maurer, M., Behringer, R., Furst, S., Thomanek, F. and Dickmanns, E. D., "A Compact Vision System for Road Vehicle Guidance Pattern Reconition," *in Proceedings of the 13th International Conference*, Vol. 4, pp. 2243-2247, 1998.

[3] Han Shue, Farrell, T., A., and Yunchun, Y., "Automatic Vehicle Steering Controls: DGPS/INS and Magnetic Markers," *in Proceedings of American Control Conference*, Vol. 1, pp. 60-65, 2003.

[4] Shladover, S., "Automated Vehicle Control Developments in the PATH Program," *IEEE Transaction on vehicular technology*, Vol. 40, No. 1, pp. 114-130, 1991.

[5] Huei, P., and Masayoshi, T., Lateral Control of Front-Wheel-Steering Rubber-Tire Vehicles, PATH Research Report, 1990.

[6] Kemin, Z., Essential of Robust Control, The first edition, Prentice-Hall, New Jersey, 1998.

[7] John, C., Keith, G., Pramod, P., and Bruce, A., "State-Space Solutions to Standard H_2 and H_∞ Control Problems," *IEEE Transactions on Automatic Control*, Vol. 34, No. 8, pp. 831-847, 1998.